

Source characteristics and along-strike variations of shallow very low frequency earthquake swarms on the Nankai Trough shallow plate boundary

Shunsuke Takemura^{1,1,1}, Satoru Baba^{1,1,1}, Suguru Yabe^{2,2,2}, Kentaro Emoto^{3,3,3}, Katsuhiko Shiomi^{4,4,4}, and Takanori Matsuzawa^{4,4,4}

¹Earthquake Research Institute, the University of Tokyo

²Geological Survey of Japan, National Institute of Advanced Industrial Science and Technology (AIST)

³Tohoku University

⁴National Research Institute for Earth Science and Disaster Resilience

November 30, 2022

Abstract

We detected shallow very low frequency earthquakes (VLFs) off the Cape Muroto and Kii Channel in the Nankai subduction zone and estimated their moment rate functions. Combining the new and previously estimated catalogs, we obtained the comprehensive catalog of shallow VLFE moment rate functions along the Nankai Trough. We defined the shallow VLFE swarms and investigated the scaling relationships of their cumulative moments, activity area, and durations in each region. Detected swarms were considered candidates for shallow slow slip events. A similar scaling relationship was observed between the cumulative moments and activity areas, irrespective of regions. It indicates similar stress drops in each region. However, the relationship between the cumulative moments and durations varied. This difference was explained by the along-strike variations in the faulting conditions of shallow slow earthquakes, such as material or hydrological properties.

Hosted file

essoar.10510250.3.docx available at <https://authorea.com/users/539748/articles/607997-source-characteristics-and-along-strike-variations-of-shallow-very-low-frequency-earthquake-swarms-on-the-nankai-trough-shallow-plate-boundary>

Shunsuke TAKEMURA¹, Satoru BABA^{1*1}, Suguru YABE², Kentaro EMOTO^{3*2},
Katsuhiko SHIOMI⁴, and Takanori MATSUZAWA⁴

¹Earthquake Research Institute, the University of Tokyo, 1-1-1 Yayoi, Bunkyo-ku, Tokyo 113-0032, Japan

²Geological Survey of Japan, National Institute of Advanced Industrial Science and Technology, Tsukuba Central 7, 1-1-1 Higashi, Tsukuba, Ibaraki 305-8567, Japan

³Geophysics, Graduate School of Science, Tohoku University, 6-3, Aramaki-aza-aoba, Aoba-ku, Sendai 980-8578, Japan

⁴National Research Institute for Earth Science and Disaster Resilience, 3-1 Tennodai, Tsukuba, Ibaraki 305-0006, Japan

Corresponding author: Shunsuke TAKEMURA (shunsuke@eri.u-tokyo.ac.jp)

Key Points:

- Comprehensive detection and source parameter estimations of shallow very low frequency earthquake swarms along the Nankai Trough.
- The scaling relationship between the activity areas and cumulative moments of the swarms roughly follows $M_o \sim A^{3/2}$.
- Along-strike variations of the scaling law for swarm durations reflect differences in the faulting conditions of slow earthquakes.

Abstract

We detected shallow very low frequency earthquakes (VLFEs) off the Cape Muroto and Kii Channel in the Nankai subduction zone and estimated their moment rate functions. Combining the new and previously estimated catalogs, we obtained the comprehensive catalog of shallow VLFE moment rate functions along the Nankai Trough. We defined the shallow VLFE swarms and investigated the scaling relationships of their cumulative moments, activity area, and durations in each region. Detected swarms were considered candidates for shallow slow slip events. A similar scaling relationship was observed between the cumulative moments and activity areas, irrespective of regions. It indicates similar stress drops in each region. However, the relationship between the cumulative moments and durations varied. This difference was explained by the along-strike variations in the faulting conditions of shallow slow earthquakes, such as material or hydrological properties.

Plain Language Summary

¹Present address: Japan Agency for Marine-Earth Science and Technology, Yokosuka Japan

²Present address: Institute of Seismology and Volcanology, Kyushu University, Fukuoka, Japan

Slow earthquakes are characterized as slips much slower than similar-size regular earthquakes. Although interactions between the shallow slow earthquakes and large tsunamigenic earthquakes have often been discussed, our knowledge of the source characteristics and spatial variations of the shallow slow earthquakes is still limited. In this study, we quantitatively investigated the activity characteristics of shallow, very low frequency earthquakes (VLFs) along the Nankai Trough. Activity areas and released cumulative moments of shallow VLFE swarms exhibited a similar scaling law irrespective of regions. However, the duration and cumulative moments of the swarms varied in each region. These characteristics can provide key information on the faulting conditions of slow earthquakes in shallow plate boundaries.

1 Introduction

Regular (fast) and slow earthquakes occur along plate boundaries in subduction zones to release the accumulated stress due to subduction (summarized in Obara & Kato, 2016; Uchida & Bürgmann, 2019). Different slip phenomena are separately distributed on the plate boundaries (e.g., Dixon et al., 2014; Nishikawa et al., 2019; Takemura, Okuwaki, et al., 2020; Vaca et al., 2018). These slips can be captured from geodetic and seismic observations. The total slips of moderate-to-large earthquakes and small repeating earthquakes can be evaluated by geodetic fault modeling (e.g., Hori et al., 2021; Okada, 1992) and empirical relationships between seismic moments and slips (e.g., Nadeau & Johnson, 1998), respectively. However, it is still difficult to evaluate small deformations due to slow slip events (SSEs), which are geodetic slips of slow earthquakes with durations of several days to years. SSEs with M_w 5.5 and 6.5 are the detectable limits in onshore and offshore regions, even when using dense Global Navigation Satellite System observations in Japan (e.g., Agata et al., 2019; Nishimura et al., 2013; Suito, 2016).

Slow earthquakes can also be observed at seismic stations. Low frequency earthquakes (LFEs) and tectonic tremors are observed in frequency ranges of 2-8 Hz (e.g., Obara, 2002). Tremors can be considered superpositions of small LFEs (e.g., Shelly et al., 2007). Very low frequency earthquakes (VLFs) are observed in the lower frequency band (0.02–0.05 Hz) (e.g., Ghosh et al., 2015; Obara & Ito, 2005). When seismic slow earthquake swarms occur simultaneously during SSEs, they are called episodic tremor and slip (ETS; Hirose & Obara, 2006; Rogers & Dragert, 2003). Small swarms of tremors and VLFs without obvious geodetic signals have often been observed around the world. Such small swarms can be considered proxies of SSEs that have M_w smaller than the detectable limits of geodetic observations. Thus, using dense onshore seismic networks, the characteristics of the swarms of deep LFEs and tremors, which occur at deeper extensions of megathrust zones, have been investigated (e.g., Aiken & Obara, 2021; Daiku et al., 2018; Frank & Brodsky, 2019; Passarelli et al., 2021). Empirical relationships between the geodetic moments of SSEs and seismic moments (or energies) of swarms have been proposed for the monitoring of slips on plate boundaries.

Slow earthquakes occur at shallower extensions of megathrust zones in the offshore regions of the Nankai subduction zone (Figure 1). Offshore observations revealed that spatiotemporal correlation of various-type shallow slow earthquake phenomena (e.g., Araki et al., 2017; Nakano et al., 2018; Yokota & Ishikawa, 2020). Because very low-frequency surface waves from shallow VLFs effectively propagate even in onshore regions and the offshore observations are still limited, long-term activities of shallow VLFs, especially in Nankai, have been investigated from onshore broadband records (e.g., Baba et al., 2020; Takemura, Matsuzawa, et al., 2019). From comparisons between their long-term catalogs and tectonic environments, shallow VLFs tend to be effectively activated by mechanical weakening due to pore fluid pressure in the areas surrounding strongly locked zones.

To obtain more detailed characteristics of shallow VLFs, Takemura et al. (2022) conducted template matching and relocation for shallow VLFs and evaluated their moment rate functions southeast of the Kii Peninsula, Japan (Regions A and B in Figure 1). Due to their techniques, estimations of epicenter locations and moment rate functions were improved from the previous catalogs (Baba et al., 2020; Takemura, Matsuzawa, et al., 2019). From the spatial distributions of the cumulative moments of shallow VLFs, they confirmed a spatial relationship between the cumulative moment of shallow VLF and the paleo-Zenisu ridge, which subducted southeast off the Kii Peninsula. In this study, we extend our previous work (Takemura et al., 2022) to off the Cape Muroto and Kii Channel (Region C in Figure 1) to reveal along-strike variations in shallow VLF activity along the Nankai Trough. Then, we investigate the source characteristics of shallow VLF swarms, which are candidates for shallow SSEs, using our new comprehensive moment-rate-function catalog of shallow VLFs along the Nankai Trough. We compare the cumulative moments of shallow VLF swarms with the geodetic moments of the corresponding shallow SSEs to discuss slip monitoring on the shallow plate boundary.

2 Data and Methods

We used broadband records from full-range seismograph network stations (F-net; Aoi et al., 2020) that are operated by the National Research Institute for Earth Science and Disaster Resilience (NIED), Japan. To avoid microseismic signals, we used a zero-phase Butterworth filter with frequencies of 0.02–0.05 Hz. The analyzed period in this study ranged from April 2004 to March 2021. The detection and relocation processes of shallow VLFs were similar to those in Takemura, Noda, et al. (2019) (see Text S1 and Figure S1 of Takemura et al., 2022). We conducted template matching analysis using template shallow VLFs (blue focal spheres in Figure 1). We divided the study area into three regions: (A) southeast of the Kii Peninsula, (B) south of the Kii Peninsula, and (C) off the Cape Muroto and Kii Channel (dashed rectangles in Figure 1).

After detection and relocation (gray circles in Figure 1), we estimated the moment rate functions of the shallow VLFs in Region C, which were constructed using a series of 6-s Küpper wavelets. The weights of each Küpper pulse were es-

timated using a Monte-Carlo-based simulated annealing method (Takemura et al., 2022). In our previous work (Takemura et al., 2022), we already estimated moment rate functions of shallow VLFES in Regions A and B. The synthetic waveforms from sources with a single 6-s Küpper pulse were evaluated by reciprocal calculations via OpenSWPC (Maeda et al., 2017) using the regional three-dimensional velocity structure model (Koketsu et al., 2012; Takemura, Yabe, et al., 2020; Tonegawa et al., 2017). Other technical details are provided in Text S1. An example of the estimated moment rate function of the shallow VLFES in Region C is illustrated in Figure S1. The fitness between the observed and synthetic waveforms improved compared to those from the previous catalog (Takemura, Matsuzawa, et al., 2019). We also compared the estimated moment rate function with the velocity waveforms of the tremor band (2–8 Hz) at N.KMTF (Figure S2) and several Hi-net stations (Figure S3). The envelope shapes of tremors typically correlate with the moment rate functions of VLFES (e.g., Ide et al., 2008; Yabe et al., 2019). Although high-frequency seismograms can be complicated due to small-scale heterogeneities and subducting oceanic plates (e.g., Furumura & Singh, 2002; Takemura et al., 2017), tremor envelopes also have multi-peak packets. This supports the longer-duration and multi-peak moment rate functions of a shallow VLFE. The shallow VLFES with moment rates of approximately 5.0×10^{12} Nm/s is the detectable lower limits (Figure 5b of Takemura et al., 2022).

According to a comparison of size distributions between Takemura et al. (2022) and Nakano et al. (2019), our catalog can stably include shallow VLFES with M_w 3.7. Spatiotemporal distributions of shallow VLFE activity are illustrated in Figure 2. The cumulative moment of shallow VLFES at each region or grid was calculated by the sum of seismic moments of shallow VLFES with variance reductions (VRs) 30 % at a certain region or grid. Our new catalog could catch larger cumulative moment releases than Takemura, Matsuzawa, et al. (2019), due to template matching and our estimation method of moment rate function, but obtained spatial variations are roughly similar as in previous studies (Takemura, Matsuzawa, et al., 2019). The relationship between shallow VLFES and tectonic environments, such as fluid and seamounts, have also been discussed in other previous studies (e.g., Sun et al., 2020; Takemura et al., 2022; Takemura, Matsuzawa, et al., 2019; Toh et al., 2020; Tonegawa et al., 2017). Then, we focus our attention on characteristics of shallow VLFE swarms. After estimating the moment rate function for shallow VLFES in region C, we combined this catalog with our previous catalog (Takemura et al., 2022; Regions A and B). From new catalog, we detected the shallow VLFE swarms in each region based on the criteria proposed by Kurihara & Obara (2021). First, we evaluated the expected inter-event times in each region by dividing the analysis period (17 y) by the total number of shallow VLFES in each region. In this study, shallow VLFE swarms were defined as more than ten consequent shallow VLFES with inter-event times shorter than the expected inter-event time in each region. Examples of shallow VLFE swarms are presented in Figure 2. The shallow VLFE episode from December 2020 was constructed by four shallow VLFE swarms in

regions A and B.

After swarm detection, we evaluated the cumulative moment, swarm duration, activity areas, and along-strike spreading distance of each shallow VLFE swarm. The swarm durations were calculated by the difference between the first and last events in each swarm. The swarm duration of A-14 is illustrated in Figure 3a. The activity areas and along-strike spreading distances were calculated using the convex hull in the Python module (red enclosed area in Figure 2b). To evaluate the cumulative moments and activity areas of the swarms, we used the shallow VLFES with VRs equal to or greater than 30%. The signals of shallow VLFES with VRs < 30 % tend to be weak compared to the noise signals. It should also be noted that because the along-dip locations of shallow VLFES have relatively large uncertainties due to station distributions (see Figures 1b and 1d of Takemura, Noda, et al., 2019, and Figure S1 of Takemura et al., 2022), their swarm areas are expected to be overestimated. The epicenter distributions in the along-dip direction seem to be roughly two times larger than those estimated using ocean bottom seismometers (Nakano et al., 2018).

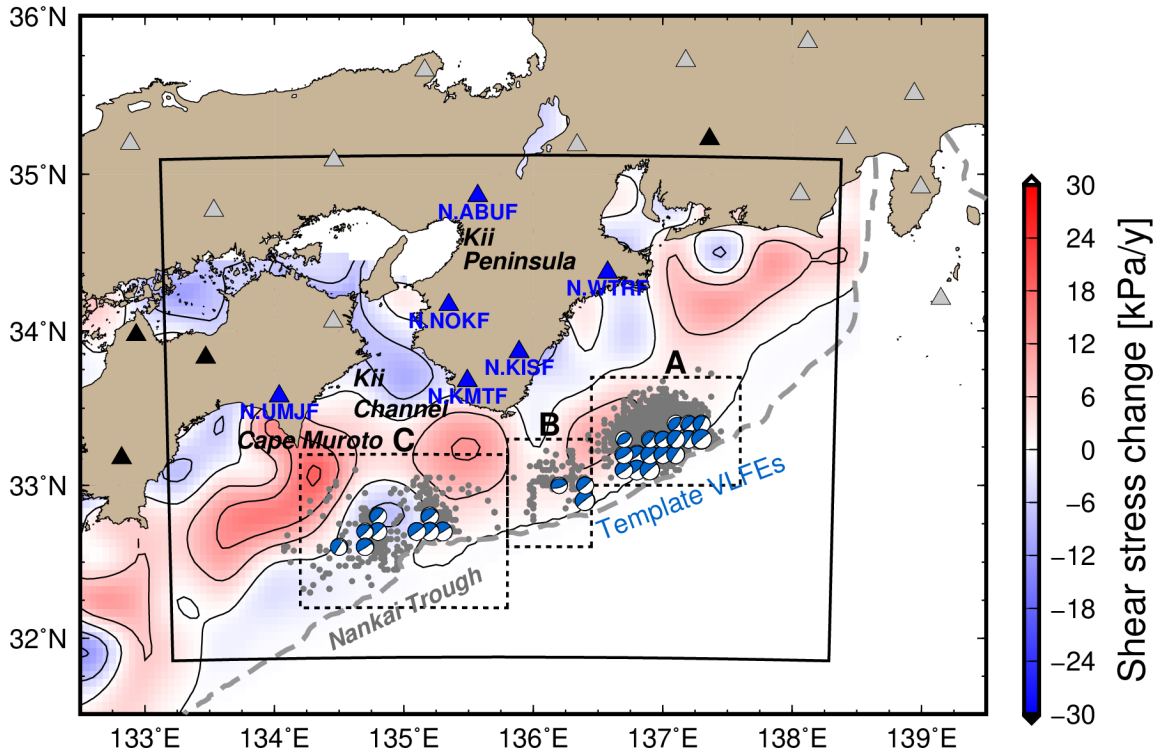


Figure 1. Map of the Nankai region. Blue focal spheres are the template shallow VLFES, which are well-constrained centroid moment tensor solutions derived from Takemura, Matsuzawa, et al. (2019). Gray circles are the epicenters of the detected shallow VLFES. Shallow VLFES in regions A and B are

from Takemura et al. (2022). Shallow VLFs in region C are from this study. Triangles denote the F-net stations. Stations with solid black and blue triangles were used for template matching and relocation. Stations represented by solid gray triangles were not used in the analysis. Moment rate function estimates for the detected VLFs were derived from the data of the solid blue triangles. The black rectangle represents the horizontal calculation region for Green's functions. Background color in the map represents the shear stress change rate due to subduction of the Philippine Sea Plate (Noda et al., 2018). The gray dashed line represents the deformation front (Nankai Trough).

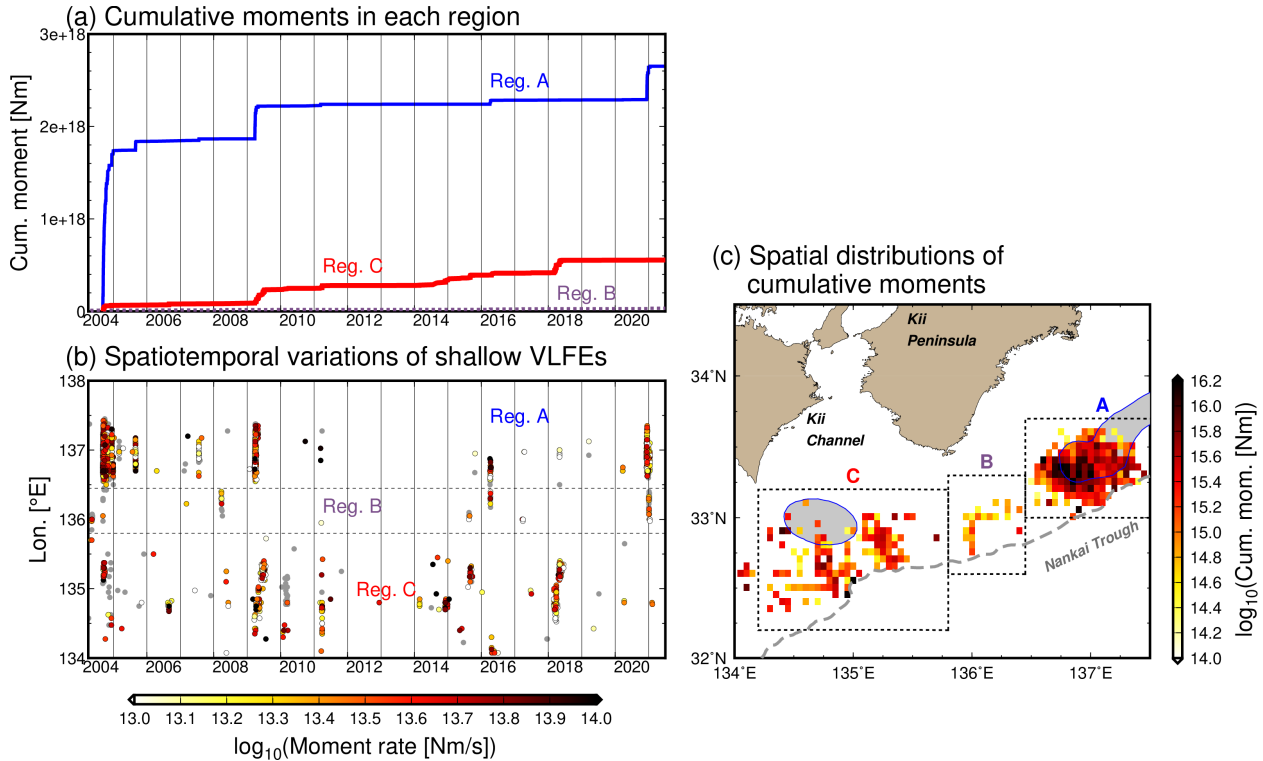


Figure 2. Spatiotemporal variations of 17 y of shallow VLFE data along the Nankai Trough. (a) Temporal variations of the cumulative moments of shallow VLFs in each region. Blue solid, purple dotted, and red bold lines are cumulative moments of shallow VLFs in regions A, B, and C, respectively. (b) Temporal variations of the along-strike shallow VLFE activity. The colors of each circle in (b) represent the moment rates of individual shallow VLFs. Gray circles represent shallow VLFs with VRs < 30%. (c) Spatial variation of cumulative moments from 17 y of shallow VLFE data. Spatial smoothing of the cumulative number and moments of shallow VLFs were conducted within the region of $0.05^\circ \times 0.05^\circ$ on the map via the gridding algorithm provided by Generic Mapping Tools (Wessel et al., 2013). The shaded areas represent the subducted seamounts around this region inferred from dense seismic surveys

(Kodaira et al., 2000; Park et al., 2004).

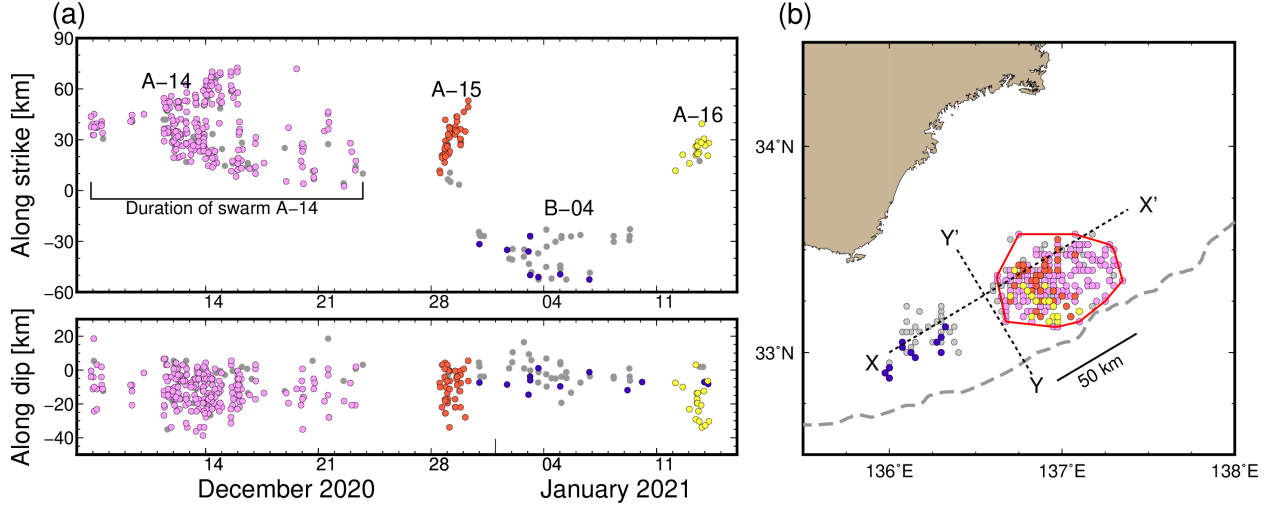


Figure 3. An example of shallow VLFE swarm detection. An example episode occurred in regions A and B from 6 December 2020 to 14 January 2021 (JST). Gray circles represent shallow VLFEs with VRs < 30%. (a) Temporal variations of shallow VLFE locations along-strike (X-X') and along-dip (Y-Y'). Colors represent swarm indices. (b) Map view of the shallow VLFE swarms from 6 December 2020 to 14 January 2021. The red enclosed area is the convex-hull of the swarm A-14. The intersection point between X-X' and Y-Y' in (b) represents X = 0 km and Y = 0 km in (a).

3 Results

We detected 16, 4, and 9 shallow VLFE swarms in regions A, B, and C, respectively (Table S1, Figure 4). The catalog of shallow VLFE including swarm index can be referred in Data Set S1. We discarded the A-01 swarm that started on September 6, 2004 (light blue square in Figure 4) since this swarm might be triggered by the M_w 7.4 intraslab earthquake and aftershocks in region A and several migrations within the similar area were confirmed (Figure S4). Figure 4a shows the relationship between the cumulative moments and areas of the shallow VLFE swarms. Although along-dip locations of the relocated shallow VLFEs had relatively large uncertainties due to station distributions, the rupture area A approximately follows a scaling law similar to regular earthquakes and deep SSEs ($Mo \propto A^{3/2}$; Gao et al., 2012; Kanamori & Brodsky, 2004). A similar scaling law between the cumulative moments and areas irrespective of the regions indicates that stress drops of the shallow VLFE swarms should be similar in all regions. Regional differences were observed in the relationship between the cumulative moments and durations of the shallow VLFE swarms. The durations of the shallow VLFE swarms in region C were almost one order larger than those in region A. It was recently reported that LFEs, and LFE clusters likely follow $Mo \propto \tau^3$ rather than $Mo \propto \tau$ (e.g., Aiken & Obara, 2021;

Supino et al., 2020). The durations of the shallow VLFE swarms in region A roughly followed Mo^{-3} , rather than Mo^{-1} . The Mo^{-1} is a typical scaling law of slow earthquake families (Ide et al., 2007). Such studies were difficult in regions B and C because of the insufficient number of shallow VLFE swarms.

Longer swarm durations in region C also indicate its slower spreading. Figure 4c shows the relationship between the cumulative moments and apparent spreading speeds, calculated by dividing the along-strike distances by each swarm duration. These speeds can be considered as the average along-strike rupture speeds of possible shallow SSEs when ruptures of possible shallow SSEs unilaterally propagate. The apparent spreading speeds in region A range from 5 to 10 km/day, corresponding to the typical migration speeds of slow earthquakes (e.g., Houston et al., 2011; Obara, 2010). Several rapid (20–30 km/day, like A-15 in Figure 2) spreadings have also been confirmed in this study. Shallow VLFE swarms in region C exhibit very slow (~1 km/day) spreading or cluster-like occurrences. Slower migrations in region C are also confirmed in Figure 2b. The apparent spreading speeds in region B are intermediate between those of regions A and C.

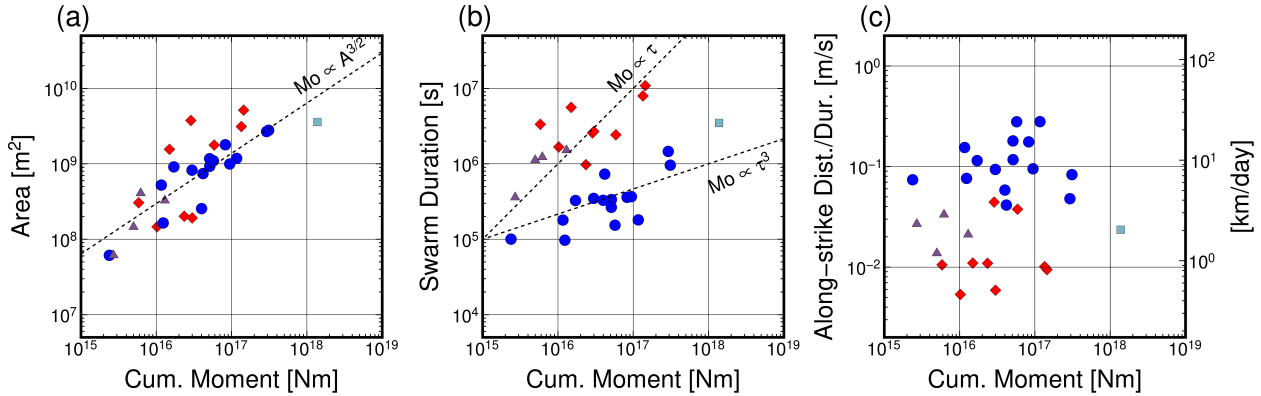


Figure 4. Scaling characteristics of shallow VLFE swarms along the Nankai Trough. Blue circles, purple triangles, and red diamonds are the resultant values in regions A, B, and C, respectively. The light blue square represents the A-01 shallow VLFE swarm that started on September 6, 2004, which can be considered as a triggered VLFE swarm due to the Mw 7.4 intraslab earthquake. Cumulative moments versus (a) swarm activity areas, (b) swarm durations, and (c) apparent spreading speeds. The apparent spreading speed was evaluated by dividing the along-strike distance by the duration of each shallow VLFE swarm. Along-strike directions were 239° in regions A and B, and 245° in region C.

4. Discussion

Spatiotemporal correlations between seismic and geodetic slow earthquakes have been found in deep slow earthquakes (e.g., Bartlow et al., 2011; Ito et al., 2007). During shallow SSE in April 2016, temporal increment in pore-fluid pressure at borehole observatory southeast off the Kii Peninsula, which reflected temporal

change in the volumetric strain due to the shallow SSE, well correlated temporal change in cumulative moments of corresponding shallow VLFES (Nakano et al., 2018). Thus, the source characteristics of the shallow VLFE swarms can correlate with those of the background shallow SSEs. According to the relationship between cumulative moments and areas of shallow VLFE swarms (Figure 4a), the stress drops of shallow SSEs are expected to be similar irrespective of regions. However, the rupture velocities of shallow SSEs are different in the three regions (Figures 4b,c). This difference might be related to differences in the faulting conditions of each region (e.g., material properties). Pore fluid pressure may also be important. Laboratory experiments show that a small change in the ratio between the average fluid pressure and the average normal stress on the fault can induce a large change in rupture velocity (Passelègue et al., 2020). Tonegawa et al. (2017, 2022) suggested that pore fluid pressure around the plate boundary in region C is expected to be higher than that in region A. Observed differences in the migration velocity may also be caused by such fluid distribution.

To obtain the broadband characteristics of shallow slow earthquakes along the Nankai Trough, we compared the cumulative moments of shallow VLFE swarms with those of corresponding shallow SSEs (Table S2). The cumulative moments of shallow VLFES were approximately 1–15 % of those of the corresponding shallow SSEs. In this comparison, we also discarded shallow VLFES with VRs < 30 %. We note that the effects of shallow VLFES with VRs < 30 % on cumulative moment evaluation are limited. We estimated the swarm areas, but we did not provide swarm stress drop estimations in this study, because static stress drop from shallow VLFE swarms are expected to be 1-15 % of the corresponding shallow SSEs.

In contrast, the cumulative moment of deep VLFES was only 0.1-1% of the corresponding deep SSEs (e.g., Ito et al., 2009; Takeo et al., 2010). Passarelli et al. (2021) investigated the seismic productivities of slow earthquakes that were calculated by dividing the cumulative seismic moments of tremors (or earthquake swarms) by the geodetic moments of the corresponding SSEs. It was observed that seismic productivity decreases with increasing depth (Figures 2 and 4 in Passarelli et al., 2021). Daiku et al. (2018) demonstrated the relationship between the seismic productivities of deep ETSs and thermal structures at depths of 30–40 km in the Nankai Trough. Thus, we think that differences in seismic productivities between the shallow and deep VLFE swarms in the Nankai Trough may be correlated with depth differences in temperature, which control the frictional and rheological properties of the faults.

A smaller number of shallow SSEs were reported (see Table S2) compared with the deep SSEs (see <http://www-solid.eps.s.u-tokyo.ac.jp/~sloweq/>; Kano et al., 2018). More shallow SSE fault models will allow us to analyze the quantitative relationship between them and VLFES. In the future, the statistical characteristics of seismic productivity of shallow slow earthquakes in each region shall be obtained. Consequently, we will quantitatively monitor slips on the shallow

plate boundary from seismic slow earthquakes (LFE, tremor, and VLFE).

5 Conclusions

Using continuous broadband records around the Nankai region, Japan, we revealed the along-strike variations in shallow VLFE activity and source characteristics of shallow VLFE swarms. Shallow VLFEs actively occur off the Cape Muroto, Kii Channel, and southeast off the Kii Peninsula (regions A and C). These spatial variations of cumulative moments from shallow VLFEs were updated and well agreed with the relationships with tectonic environments in previous studies. Heterogeneous stress and structural properties due to the subducted seamounts promote shallow slow earthquakes along the Nankai Trough.

We investigated the shallow VLFE swarms in each region, which could be candidates for shallow SSEs. We conclude that the cumulative moments and activity areas of shallow VLFE swarms follow a similar scaling law irrespective of region, indicated by similar stress drop values. However, relationships between the cumulative moments and durations of the shallow VLFE swarms vary in each region. The apparent spreading speeds are also variable characteristics. These differences can be explained by regional differences in the faulting conditions of the shallow slow earthquakes, such as material or hydrological properties.

Acknowledgments

Numerical simulations for evaluating the Green’s functions were conducted using the Fujitsu PRIMERGY CX600M1/CX1640M1 (Oakforest-PAC) at the Information Technology Center, University of Tokyo. This study was supported by a JSPS KAKENHI Grant-in-Aid for Scientific Research (C), grant number JP21K03696, and a Grant-in-Aid for Scientific Research on Transformative Research Areas “Science of Slow-to-Fast earthquakes,” grant numbers JP21H05200, JP21H05203, JP21H05205, and JP21H05206. This study was also supported by ERI JURP 2021-S-B102, which provided the computational resources for calculating the Green’s functions. We also acknowledge Dr. Baoning Wu, an anonymous reviewer and editor Prof. Germán Prieto, for careful reviewing and constructive comments, which helped to improve the manuscript.

Data availability statement

The Python package HinetPy (Tian, 2020) was used to download the NIED F-net/Hi-net continuous records (National Research Institute for Earth Science and Disaster Resilience, 2019a, 2019b). We simulated the Green’s functions in the local 3D model using OpenSWPC version 5.1.0 <https://doi.org/10.5281/zenodo.3982232>. The modified 1D layered velocity models of Tonegawa et al. (2017) can be downloaded from <https://doi.org/10.5281/zenodo.4158947>. The model of Koketsu et al. (2012) was obtained from https://www.jishin.go.jp/evaluation/seismic_hazard_map/lpshm/12_choshuki_dat/. We used the seismic analysis code (Goldstein & Snoke, 2005; Helffrich et al., 2013) and generic mapping tools (Wessel et al., 2013) for signal processing and figure drawing. Data analysis was conducted using NumPy (Harris et al., 2020), SciPy

1.7.0 (<https://doi.org/10.5281/zenodo.5000479>), and Pandas 1.2.5 (<https://doi.org/10.5281/zenodo.5013202>). The estimated moment rate functions of shallow VLFs along the Nankai Trough can be downloaded from <https://doi.org/10.5281/zenodo.5211090> and <https://doi.org/10.5281/zenodo.5824418>.

References

Agata, R., Hori, T., Ariyoshi, K., & Ichimura, T. (2019). Detectability analysis of interplate fault slips in the Nankai subduction thrust using seafloor observation instruments. *Marine Geophysical Research*. <https://doi.org/10.1007/s11001-019-09380-y>

Aiken, C., & Obara, K. (2021). Data-Driven Clustering Reveals More Than 900 Small Magnitude Slow Earthquakes and Their Characteristics. *Geophysical Research Letters*, *48*(11). <https://doi.org/10.1029/2020GL091764>

Aoi, S., Asano, Y., Kunugi, T., Kimura, T., Uehira, K., Takahashi, N., et al. (2020). MOWLAS: NIED observation network for earthquake, tsunami and volcano. *Earth, Planets and Space*, *72*(1). <https://doi.org/10.1186/s40623-020-01250-x>

Araki, E., Saffer, D. M., Kopf, A. J., Wallace, L. M., Kimura, T., Machida, Y., et al. (2017). Recurring and triggered slow-slip events near the trench at the Nankai Trough subduction megathrust. *Science*, *356*(6343), 1157–1160. <https://doi.org/10.1126/science.aan3120>

Baba, S., Takemura, S., Obara, K., & Noda, A. (2020). Slow earthquakes illuminating interplate coupling heterogeneities in subduction zones. *Geophysical Research Letters*, 4–5. <https://doi.org/10.1029/2020gl088089>

Bartlow, N. M., Miyazaki, S., Bradley, A. M., & Segall, P. (2011). Space-time correlation of slip and tremor during the 2009 Cascadia slow slip event. *Geophysical Research Letters*, *38*(18), 1–6. <https://doi.org/10.1029/2011GL048714>

Daiku, K., Hiramatsu, Y., Matsuzawa, T., & Mizukami, T. (2018). Slow slip rate and excitation efficiency of deep low-frequency tremors beneath southwest Japan. *Tectonophysics*, *722*(May 2017), 314–323. <https://doi.org/10.1016/j.tecto.2017.11.016>

Dixon, T. H., Jiang, Y., Malservisi, R., McCaffrey, R., Voss, N., Protti, M., & Gonzalez, V. (2014). Earthquake and tsunami forecasts: Relation of slow slip events to subsequent earthquake rupture. *Proceedings of the National Academy of Sciences*, *111*(48), 17039–17044. <https://doi.org/10.1073/pnas.1412299111>

Frank, W. B., & Brodsky, E. E. (2019). Daily measurement of slow slip from low-frequency earthquakes is consistent with ordinary earthquake scaling, (October), 1–7.

Furumura, T., & Singh, S. K. (2002). Regional wave propagation from Mexican subduction zone earthquakes: The attenuation functions for interplate and slab events. *Bulletin of the Seismological Society of America*, *92*(6), 2110–2125.

<https://doi.org/10.1785/0120010278>

Gao, H., Schmidt, D. A., & Weldon, R. J. (2012). Scaling Relationships of Source Parameters for Slow Slip Events. *Bulletin of the Seismological Society of America*, *102*(1), 352–360. <https://doi.org/10.1785/0120110096>

Ghosh, A., Huesca-Pérez, E., Brodsky, E., & Ito, Y. (2015). Very low frequency earthquakes in Cascadia migrate with tremor. *Geophysical Research Letters*, *42*(9), 3228–3232. <https://doi.org/10.1002/2015GL063286>

Goldstein, P., & Snoko, A. (2005). SAC Availability for the IRIS Community. Retrieved from <https://ds.iris.edu/ds/newsletter/vol7/no1/193/sac-availability-for-the-iris-community/>

Harris, C. R., Millman, K. J., van der Walt, S. J., Gommers, R., Virtanen, P., Cournapeau, D., et al. (2020). Array programming with NumPy. *Nature*, *585*(7825), 357–362. <https://doi.org/10.1038/s41586-020-2649-2>

Helfrich, G., Wookey, J., & Bastow, I. (2013). *The Seismic Analysis Code*. Cambridge: Cambridge University Press. <https://doi.org/10.1017/CBO9781139547260>

Hirose, H., & Obara, K. (2006). Short-term slow slip and correlated tremor episodes in the Tokai region, central Japan. *Geophysical Research Letters*, *33*(17), L17311. <https://doi.org/10.1029/2006GL026579>

Hori, T., Agata, R., Ichimura, T., Fujita, K., Yamaguchi, T., & Iinuma, T. (2021). High-fidelity elastic Green’s functions for subduction zone models consistent with the global standard geodetic reference system. *Earth, Planets and Space*, *73*(1). <https://doi.org/10.1186/s40623-021-01370-y>

Houston, H., Delbridge, B. G., Wech, A. G., & Creager, K. C. (2011). Rapid tremor reversals in Cascadia generated by a weakened plate interface. *Nature Geoscience*, *4*(6), 404–409. <https://doi.org/10.1038/ngeo1157>

Ide, S., Beroza, G. C., Shelly, D. R., & Uchide, T. (2007). A scaling law for slow earthquakes. *Nature*, *447*(7140), 76–79. <https://doi.org/10.1038/nature05780>

Ide, S., Imanishi, K., Yoshida, Y., Beroza, G. C., & Shelly, D. R. (2008). Bridging the gap between seismically and geodetically detected slow earthquakes. *Geophysical Research Letters*, *35*(10), 2–7. <https://doi.org/10.1029/2008GL034014>

Ito, Y., Obara, K., Shiomi, K., Sekine, S., & Hirose, H. (2007). Slow earthquakes coincident with episodic tremors and slow slip events. *Science*, *315*(5811), 503–506. <https://doi.org/10.1126/science.1134454>

Ito, Y., Obara, K., Matsuzawa, T., & Maeda, T. (2009). Very low frequency earthquakes related to small asperities on the plate boundary interface at the locked to aseismic transition. *Journal of Geophysical Research: Solid Earth*, *114*(B11), 1–16. <https://doi.org/10.1029/2008JB006036>

Kanamori, H., & Brodsky, E. E. (2004). The physics of earthquakes. *Reports on Progress in Physics*, *67*(8), 1429–1496. <https://doi.org/10.1088/0034->

4885/67/8/R03

- Kano, M., Aso, N., Matsuzawa, T., Ide, S., Annoura, S., Arai, R., et al. (2018). Development of a slow earthquake database. *Seismological Research Letters*, 89(4), 1566–1575. <https://doi.org/10.1785/0220180021>
- Kodaira, S., Takahashi, N., Nakanishi, A., Miura, S., & Kaneda, Y. (2000). Subducted seamount imaged in the rupture zone of the 1946 Nankaido earthquake. *Science*, 289(5476), 104–106. <https://doi.org/10.1126/science.289.5476.104>
- Koketsu, K., Miyake, H., & Suzuki, H. (2012). Japan Integrated Velocity Structure Model Version 1. *Proceedings of the 15th World Conference on Earthquake Engineering*, 1–4. Retrieved from http://www.iitk.ac.in/nicee/wcee/article/WCEE2012_1773.pdf
- Kurihara, R., & Obara, K. (2021). Spatiotemporal Characteristics of Relocated Deep Low-Frequency Earthquakes Beneath 52 Volcanic Regions in Japan Over an Analysis Period of 14 Years and 9 Months. *Journal of Geophysical Research: Solid Earth*, 126(10). <https://doi.org/10.1029/2021JB022173>
- Maeda, T., Takemura, S., & Furumura, T. (2017). OpenSWPC: An open-source integrated parallel simulation code for modeling seismic wave propagation in 3D heterogeneous viscoelastic media.
- Nadeau, R. M., & Johnson, J. R. (1998). Seismological Studies at Parkfield IV: Moment Release Rates and Estimates of Source Parameters for Small Repeating Earthquakes. *Bull. Seis. Soc. Am.*, 88(3), 790–814.
- Nakano, M., Hori, T., Araki, E., Kodaira, S., & Ide, S. (2018). Shallow very-low-frequency earthquakes accompany slow slip events in the Nankai subduction zone. *Nature Communications*, 9(1), 984. <https://doi.org/10.1038/s41467-018-03431-5>
- Nakano, M., Yabe, S., Sugioka, H., Shinohara, M., & Ide, S. (2019). Event Size Distribution of Shallow Tectonic Tremor in the Nankai Trough. *Geophysical Research Letters*, 46(11), 5828–5836. <https://doi.org/10.1029/2019GL083029>
- National Research Institute for Earth Science and Disaster Resilience. (2019a). NIED F-net. <https://doi.org/10.17598/NIED.0005>
- National Research Institute for Earth Science and Disaster Resilience. (2019b). NIED Hi-net. <https://doi.org/10.17598/NIED.0003>
- Nishikawa, T., Matsuzawa, T., Ohta, K., Uchida, N., Nishimura, T., & Ide, S. (2019). The slow earthquake spectrum in the Japan Trench illuminated by the S-net seafloor observatories. *Science*, 365(August), 808–813. <https://doi.org/10.1126/science.aax5618>
- Nishimura, T., Matsuzawa, T., & Obara, K. (2013). Detection of short-term slow slip events along the Nankai Trough, southwest Japan, using GNSS data. *Journal of Geophysical Research: Solid Earth*, 118(6), 3112–3125. <https://doi.org/10.1002/jgrb.50222>

- Noda, A., Saito, T., & Fukuyama, E. (2018). Slip-Deficit Rate Distribution Along the Nankai Trough, Southwest Japan, With Elastic Lithosphere and Viscoelastic Asthenosphere. *Journal of Geophysical Research: Solid Earth*, *123*(9), 8125–8142. <https://doi.org/10.1029/2018JB015515>
- Obara, K. (2002). Nonvolcanic deep tremor associated with subduction in southwest Japan. *Science*, *296*(5573), 1679–1681. <https://doi.org/10.1126/science.1070378>
- Obara, K. (2010). Phenomenology of deep slow earthquake family in southwest Japan: Spatiotemporal characteristics and segmentation. *Journal of Geophysical Research: Solid Earth*, *115*(8), 1–22. <https://doi.org/10.1029/2008JB006048>
- Obara, K., & Ito, Y. (2005). Very low frequency earthquakes excited by the 2004 off Kii peninsula earthquakes: A dynamic deformation process in the large accretionary prism. *Earth, Planets and Space*, *57*(4), 321–326. <https://doi.org/10.1186/BF03352570>
- Obara, K., & Kato, A. (2016). Connecting slow earthquakes to huge earthquakes. *Science*, *353*(6296), 253–257. <https://doi.org/10.1126/science.aaf1512>
- Okada, Y. (1992). Internal Deformation due to Shear and Tensile Faults in a Half-space. *Bulletin of the Seismological Society of America*, *82*(2), 1018–1040.
- Park, J.-O., Moore, G. F., Tsuru, T., Kodaira, S., & Kaneda, Y. (2004). A subducted oceanic ridge influencing the Nankai megathrust earthquake rupture. *Earth and Planetary Science Letters*, *217*(1–2), 77–84. [https://doi.org/10.1016/S0012-821X\(03\)00553-3](https://doi.org/10.1016/S0012-821X(03)00553-3)
- Passarelli, L., Selvadurai, P. A., Rivalta, E., & Jónsson, S. (2021). The source scaling and seismic productivity of slow slip transients. *Science Advances*, *7*(32). <https://doi.org/10.1126/sciadv.abg9718>
- Passelègue, F. X., Almakari, M., Dublanchet, P., Barras, F., Fortin, J., & Violay, M. (2020). Initial effective stress controls the nature of earthquakes. *Nature Communications*, *11*(1), 1–8. <https://doi.org/10.1038/s41467-020-18937-0>
- Rogers, G., & Dragert, H. (2003). Episodic tremor and slip on the Cascadia subduction zone: the chatter of silent slip. *Science*, *300*(5627), 1942–1943. <https://doi.org/10.1126/science.1084783>
- Shelly, D. R., Beroza, G. C., & Ide, S. (2007). Non-volcanic tremor and low-frequency earthquake swarms. *Nature*, *446*(7133), 305–307. <https://doi.org/10.1038/nature05666>
- Suito, H. (2016). Detectability of Interplate Fault Slip around Japan, Based on GEONET Daily Solution F3 (in Japanese with English abstract). *Journal of the Geodetic Society of Japan*, *62*(3), 109–120. <https://doi.org/10.11366/sokuchi.62.109>
- Sun, T., Saffer, D., & Ellis, S. (2020). Mechanical and hydrological effects of seamount subduction on megathrust stress and slip. *Nature Geoscience*, *13*(March). <https://doi.org/10.1038/s41561-020-0542-0>

- Supino, M., Poiata, N., Festa, G., Vilotte, J. P., Satriano, C., & Obara, K. (2020). Self-similarity of low-frequency earthquakes. *Scientific Reports*, *10*(1), 1–9. <https://doi.org/10.1038/s41598-020-63584-6>
- Takemura, S., Kobayashi, M., & Yoshimoto, K. (2017). High-frequency seismic wave propagation within the heterogeneous crust: effects of seismic scattering and intrinsic attenuation on ground motion modelling. *Geophysical Journal International*, *210*(3), 1806–1822. <https://doi.org/10.1093/gji/ggx269>
- Takemura, S., Noda, A., Kubota, T., Asano, Y., Matsuzawa, T., & Shiomi, K. (2019). Migrations and Clusters of Shallow Very Low Frequency Earthquakes in the Regions Surrounding Shear Stress Accumulation Peaks Along the Nankai Trough. *Geophysical Research Letters*, *46*(21), 11830–11840. <https://doi.org/10.1029/2019GL084666>
- Takemura, S., Matsuzawa, T., Noda, A., Tonegawa, T., Asano, Y., Kimura, T., & Shiomi, K. (2019). Structural Characteristics of the Nankai Trough Shallow Plate Boundary Inferred From Shallow Very Low Frequency Earthquakes. *Geophysical Research Letters*, *46*(8), 4192–4201. <https://doi.org/10.1029/2019GL082448>
- Takemura, S., Okuwaki, R., Kubota, T., Shiomi, K., Kimura, T., & Noda, A. (2020). Centroid moment tensor inversions of offshore earthquakes using a three-dimensional velocity structure model: slip distributions on the plate boundary along the Nankai Trough. *Geophysical Journal International*, *222*(2), 1109–1125. <https://doi.org/10.1093/gji/ggaa238>
- Takemura, S., Yabe, S., & Emoto, K. (2020). Modelling high-frequency seismograms at ocean bottom seismometers: effects of heterogeneous structures on source parameter estimation for small offshore earthquakes and shallow low-frequency tremors. *Geophysical Journal International*, *223*(3), 1708–1723. <https://doi.org/10.1093/gji/ggaa404>
- Takemura, S., Obara, K., Shiomi, K., & Baba, S. (2022). Spatiotemporal Variations of Shallow Very Low Frequency Earthquake Activity Southeast Off the Kii Peninsula, Along the Nankai Trough, Japan. *Journal of Geophysical Research: Solid Earth*, *127*(3), e2021JB023073. <https://doi.org/10.1029/2021JB023073>
- Takeo, A., Idehara, K., Iritani, R., Tonegawa, T., Nagaoka, Y., Nishida, K., et al. (2010). Very broadband analysis of a swarm of very low frequency earthquakes and tremors beneath Kii Peninsula, SW Japan. *Geophysical Research Letters*, *37*(6), n/a-n/a. <https://doi.org/10.1029/2010GL042586>
- Tian, D. (2020). HinetPy: A Python package to request and process seismic waveform data from Hi-net. <https://doi.org/10.5281/zenodo.3885779>
- Toh, A., Chen, W. J., Takeuchi, N., Dreger, D. S., Chi, W. C., & Ide, S. (2020). Influence of a Subducted Oceanic Ridge on the Distribution of Shallow VLFs in the Nankai Trough as Revealed by Moment Tensor

- Inversion and Cluster Analysis. *Geophysical Research Letters*, 47(15), 0–3. <https://doi.org/10.1029/2020GL087244>
- Tonegawa, T., Araki, E., Kimura, T., Nakamura, T., Nakano, M., & Suzuki, K. (2017). Sporadic low-velocity volumes spatially correlate with shallow very low frequency earthquake clusters. *Nature Communications*, 8(1), 2048. <https://doi.org/10.1038/s41467-017-02276-8>
- Tonegawa, T., Takemura, S., Yabe, S., & Yomogida, K. (2022). Fluid migration before and during slow earthquakes in the shallow Nankai subduction zone. *Journal of Geophysical Research: Solid Earth*. <https://doi.org/10.1029/2021JB023583>
- Uchida, N., & Bürgmann, R. (2019). Repeating Earthquakes. *Annual Review of Earth and Planetary Sciences*, 47(1), 305–332. <https://doi.org/10.1146/annurev-earth-053018-060119>
- Vaca, S., Vallée, M., Nocquet, J. M., Battaglia, J., & Régnier, M. (2018). Recurrent slow slip events as a barrier to the northward rupture propagation of the 2016 Pedernales earthquake (Central Ecuador). *Tectonophysics*, 724–725(November 2017), 80–92. <https://doi.org/10.1016/j.tecto.2017.12.012>
- Wessel, P., Smith, W. H. F., Scharroo, R., Luis, J., & Wobbe, F. (2013). Generic mapping tools: Improved version released. *Eos*, 94(45), 409–410. <https://doi.org/10.1002/2013EO450001>
- Yabe, S., Tonegawa, T., & Nakano, M. (2019). Scaled Energy Estimation for Shallow Slow Earthquakes. *Journal of Geophysical Research: Solid Earth*, 124(2), 1507–1519. <https://doi.org/10.1029/2018JB016815>
- Yokota, Y., & Ishikawa, T. (2020). Shallow slow slip events along the Nankai Trough detected by GNSS-A. *Science Advances*, 6(3), eaay5786. <https://doi.org/10.1126/sciadv.aay5786>

Geophysical Research Letters

Supporting Information for

Source characteristics and along-strike variations of shallow very low frequency earthquake swarms along the Nankai Trough

Shunsuke TAKEMURA¹, Satoru BABA^{1*a}, Suguru YABE², Kentaro EMOTO^{3*b},
Katsuhiko SHIOMI⁴, and Takanori MATSUZAWA⁴

¹Earthquake Research Institute, the University of Tokyo, 1-1-1 Yayoi, Bunkyo-ku, Tokyo 113-0032, Japan

²Geological Survey of Japan, National Institute of Advanced Industrial Science and Technology, Tsukuba Central 7, 1-1-1 Higashi, Tsukuba, Ibaraki 305-8567, Japan

³Geophysics, Graduate School of Science, Tohoku University, 6-3, Aramaki-aza-aoba, Aoba-ku, Sendai 980-8578, Japan

⁴National Research Institute for Earth Science and Disaster Resilience, 3-1 Tennodai, Tsukuba, Ibaraki 305-0006, Japan

Contents of this file

Text S1

Figures S1 to S4

Tables S1 and S2

Additional Supporting Information (Files uploaded separately)

Captions for Figure S1 to S4

Captions for Tables S1 and S2

Introduction

^a Present address: Japan Agency for Marine-Earth Science and Technology, Yokosuka Japan

^b Present address: Institute of Seismology and Volcanology, Kyushu University, Fukuoka, Japan

The methods for the detection and moment rate function estimation are described in Text S1. Figure S1 shows an example of the resultant moment rate function for a shallow VLFE. Figures S2 and S3 are comparative plots of the estimated moment rate functions and filtered velocity envelopes with frequencies of 2–8 Hz. Spatiotemporal variations of shallow VLFEs in the A-1, A-2, and A-3 swarms are illustrated in Figure S4. Particularly, the A-1 swarm is considered to be triggered by the Mw 7.4 intra-slab earthquake. The source characteristics of the shallow VLFE swarms are listed in Table S1. Table S2 shows the comparisons between the shallow SSEs and the corresponding swarms.

Text S1.

To detect the shallow very low frequency earthquakes (VLFs), we calculated the cross-correlation coefficients (CCs) between the filtered template and observed seismograms every 1 s. We employed the 2nd order zero-phase Butterworth filter in the frequency range of 0.02–0.05 Hz. The blue focal spheres in Figure 1 show the template events of the shallow VLFs. Template waveforms can be downloaded from Takemura, Noda, et al. (2019). Assuming 3.8 km/s as the propagation velocity of surface wave, the CCs at the stations were back-propagated to possible shallow VLF epicenters, which were uniformly distributed at an interval of 0.025° on the plate boundary. We detected the events with station-averaged CCs ≥ 0.45 as shallow VLF candidates. To avoid regular earthquakes and duplicate detections, we removed the local regular earthquakes listed in the unified hypocenter catalog of the Japan Meteorological Agency. We selected a shallow VLF candidate with a maximum CC every 60 s.

We estimated the moment rate functions of the detected shallow VLFs using a Monte Carlo-based simulated annealing technique. An open-source seismic wave propagation code (OpenSWPC; Maeda et al., 2017) was used for the calculation of the Green's function. The simulation model covered an area of $360 \times 480 \times 80 \text{ km}^3$ (black rectangle in Figure 1), discretized by grid intervals of 0.2 km in the horizontal direction and 0.1 km in the vertical direction. The 3D velocity model was constructed by combining the Japan Integrated Velocity Structure Model (JIVSM Koketsu et al., 2012) and 1D velocity models beneath the DONET stations (<https://doi.org/10.5281/zenodo.4158946> Tonegawa et al., 2017). The detailed model construction process is described in Takemura et al. (2020). The possible source grids were distributed at an interval of 0.025° .

The moment rate function was estimated as follows: The epicenters and depths were fixed as relocation results and the depth of the upper surface of the Philippine Sea Plate. Previous studies have revealed that shallow VLFs can be modeled as low-angle thrust faults on the plate boundary (e.g., Sugioka et al., 2012; Takemura et al., 2018). Thus, focal mechanisms were assumed to be low-angle thrust faults constructed by the plate geometry of JIVSM and the convergence directions of NUVEL-1A (DeMets et al., 2010). The moment rate function was constructed using a series of Küpper wavelets with a duration of 6 s. The synthetic velocity waveform $v_{ij}(t)$ from the j -th source grid to the i -th station can be written as follows:

$$v_{ij}(t) = A_0 \sum_{k=0}^{N_p-1} w_k^2 G_{ij}(t - k\Delta t)$$

where G_{ij} is the Green's function of the j -th source with a 6-s Küpper wavelet, w_k^2 is the weight of the k -th Küpper wavelet, and Δt is the offset of each pulse (3 s). Non-negative conditions (w_k^2) were imposed in our estimation. A_0 is the optimal relative amplitude

estimated by fitting the observed waveforms to synthetic waveforms based on variance reduction (e.g., Yabe et al., 2021). Using the observed waveform and amplitude-adjusted model seismogram v^{syn} , the objective function used in this analysis is as follows:

$$E = \sum_i \sum_l |v_{ij}^{obs}(t_l + \tau) - v_{ij}^{syn}(t_l)|$$

where τ is the delay time and the length of the time window is 200 s ($t_l = 0\text{--}200$ s). The parameters w_k^2 and τ were estimated using a Monte Carlo-based simulated annealing procedure. $\Delta w = 0.02$ and $\Delta \tau = 0.5$ s were perturbed at each time step for the source weights (w_k) and delay time (τ), respectively. According to shallow VLFE duration measurements derived from offshore broadband analysis (Sugioka et al., 2012), the number of source weight parameters was 40; thus, the maximum duration of the modeled moment rate function was 123 s.

The initial temperature and cooling rate in the simulated annealing were $T_0 = 3E_0$ and $\gamma = 0.996$, respectively (e.g., Tocheport et al., 2007). We initially assumed $w_k^2 = 1$, which was not able to reproduce the observed seismograms (Figure 2b). $T_k = \gamma^k T_0$ gives the annealing schedule at the k -th iteration. The perturbation at the k -th iteration with $\Delta E_k (= E_k - E_{k-1}) < 0$ was fully accepted. We also accepted the perturbation with $\Delta E_k \geq 0$ and the probability of $P = \exp(-\Delta E_k / T_k)$ equal to less than α , which is a random number between 0 and 1 at each iteration.

The estimations were conducted using a frequency band of 0.02–0.05 Hz to avoid the effects of microseisms at onshore stations (e.g., Nishida, 2017). In some cases, the resultant moment rate functions have longer-duration late moment releases, which do not contribute to the reproducibility of observed shallow VLFE signals with frequencies of 0.02–0.05 Hz (e.g., Figure 2 of Takemura et al., 2021). Due to such band-limited analysis, we could not distinguish whether the longer-duration late moment release in the simulated annealing result was a source energy release or an artifact (Figure S3 of Takemura et al., 2021). Additionally, our method might model the reverberations of later weak surface waves within the oceanic sediments and noise signals as a seismic moment release from the source for cases with a low signal-to-noise ratio. Therefore, to avoid misestimating the moment rate functions after simulated annealing, especially due to noise signals, we calculated the variance reductions (VRs) between the observed and synthetic seismograms that were constructed using N Küpper pulses. We adopted the N -th ($N = 1\text{--}40$) parameters, which achieved 90% of the maximum VR (VR_m) for simulated annealing. Several thresholds were tested in a previous study (Takemura et al., 2021).

After obtaining the optimal solution, we calculated the VR values between the observed and optimal synthetic seismograms. These VR values represented the goodness-of-fit factors for the optimal solutions. For shallow VLFs with lower VRs (<30%), the signals at onshore F-net stations could be weak compared to the noise signals; consequently, their durations might be misestimated due to low signal-to-noise ratio

conditions. Therefore, in subsequent discussions of shallow VLFE activities, we discarded the results with VRs <30%.

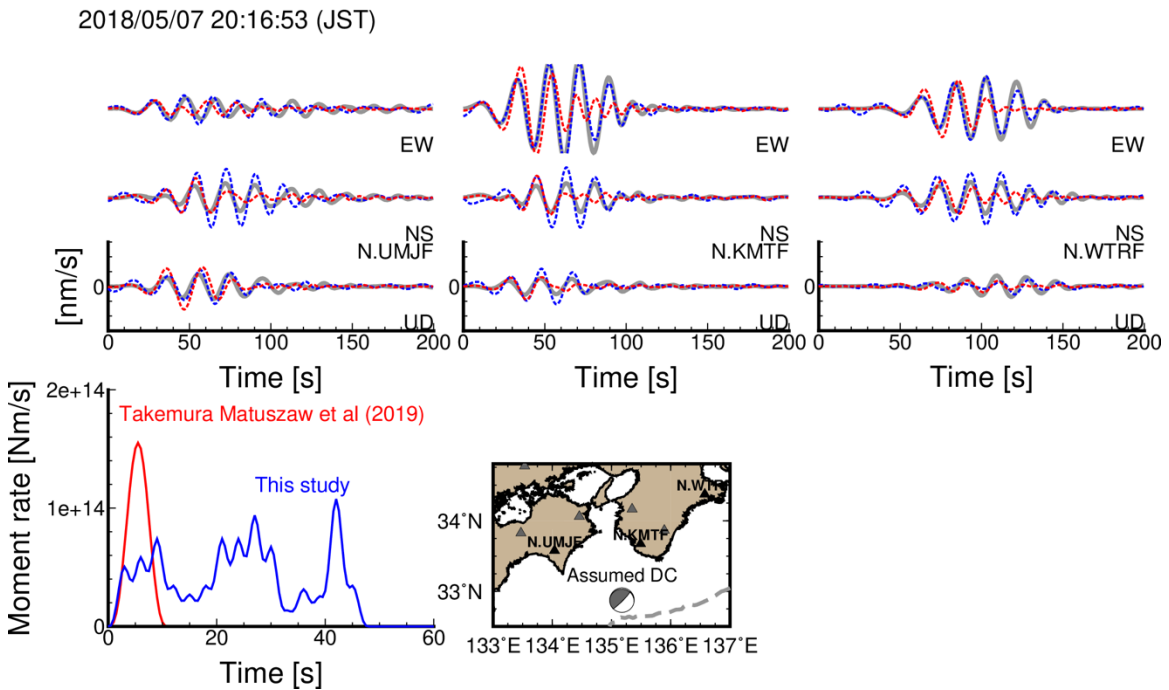


Figure S1. Comparison of estimated moment rate functions between this study (blue lines) and a previous study (red lines, Takemura, Matsuzawa, et al., 2019). In the upper panel, gray, red, and blue lines represent the observed waveforms, synthetic waveforms of Takemura, Matsuzawa, et al. (2019), and synthetic waveforms of this study, respectively. A band-pass filter of 0.02–0.05 Hz was applied. Station locations are shown on the map. Estimated moment rate functions are illustrated in the left bottom panel. Estimated seismic moments of Takemura, Matsuzawa, et al. (2019) and this study are 7.24×10^{14} and 2.04×10^{15} Nm, respectively.

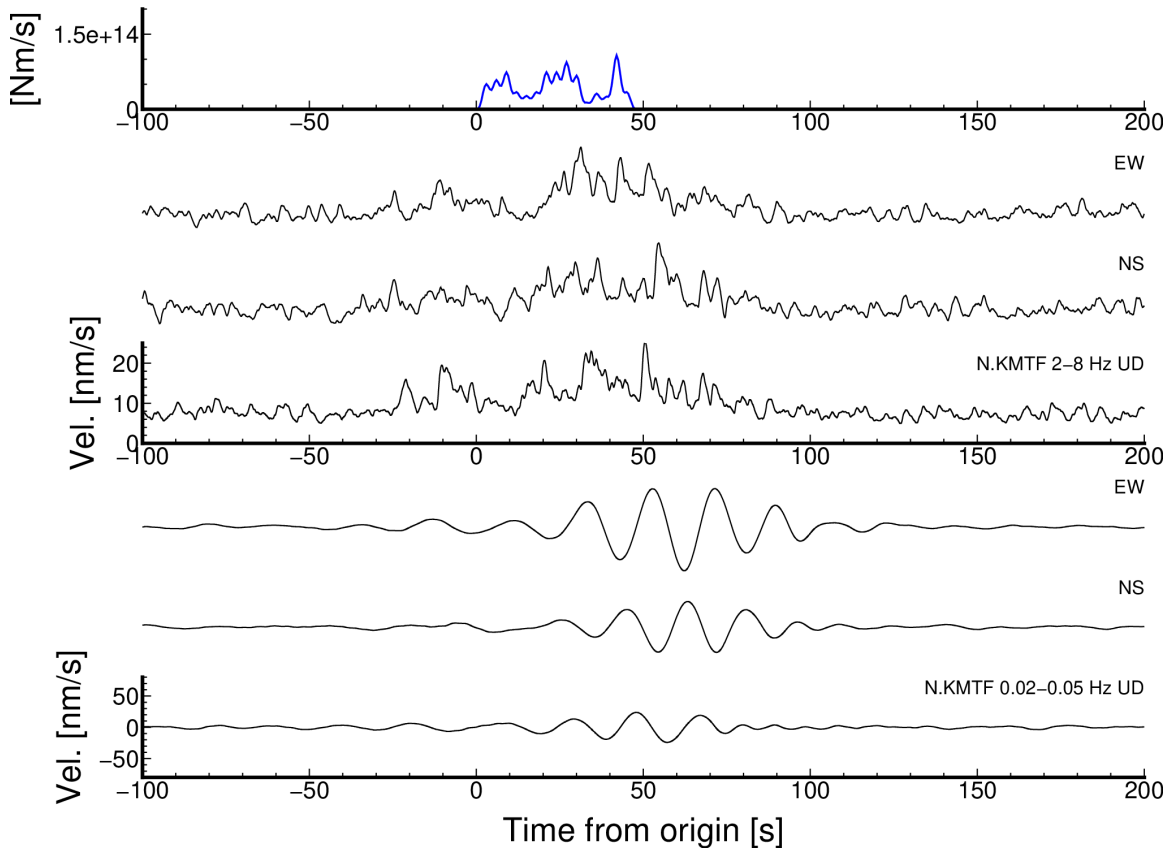


Figure S2. Comparison of low-frequency waveforms and high-frequency envelopes at N.KMTF during a shallow VLFE occurred at 20:16:53 on May 7, 2018 (JST). We also plotted the estimated moment rate function of a shallow VLFE (blue line) in the upper panel.

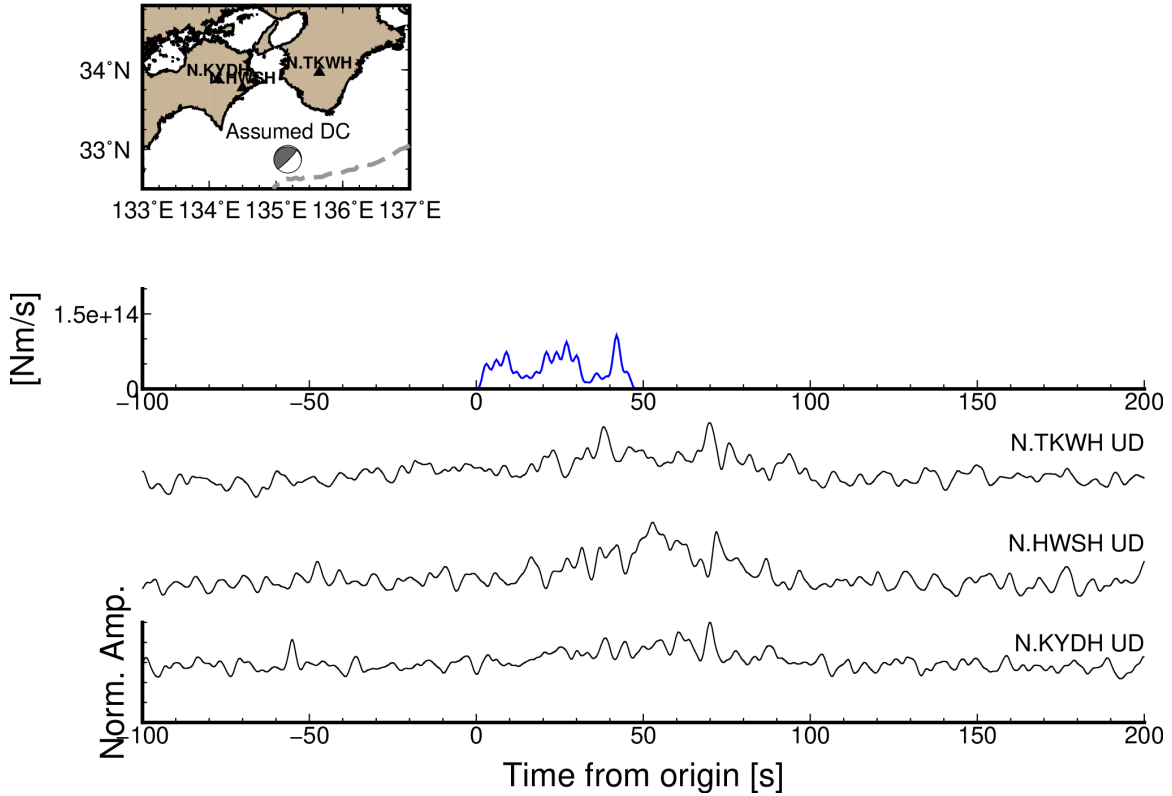


Figure S3. Examples of high-frequency (2–8 Hz) envelopes of vertical velocity seismograms at Hi-net (National Research Institute for Earth Science and Disaster Resilience, 2019) stations during a shallow VLFE that occurred at 20:16:53 on May 7, 2018 (JST). We also plotted the estimated moment rate function of a shallow VLFE (blue line) in the upper panel. Locations of used Hi-net stations are shown in the map.

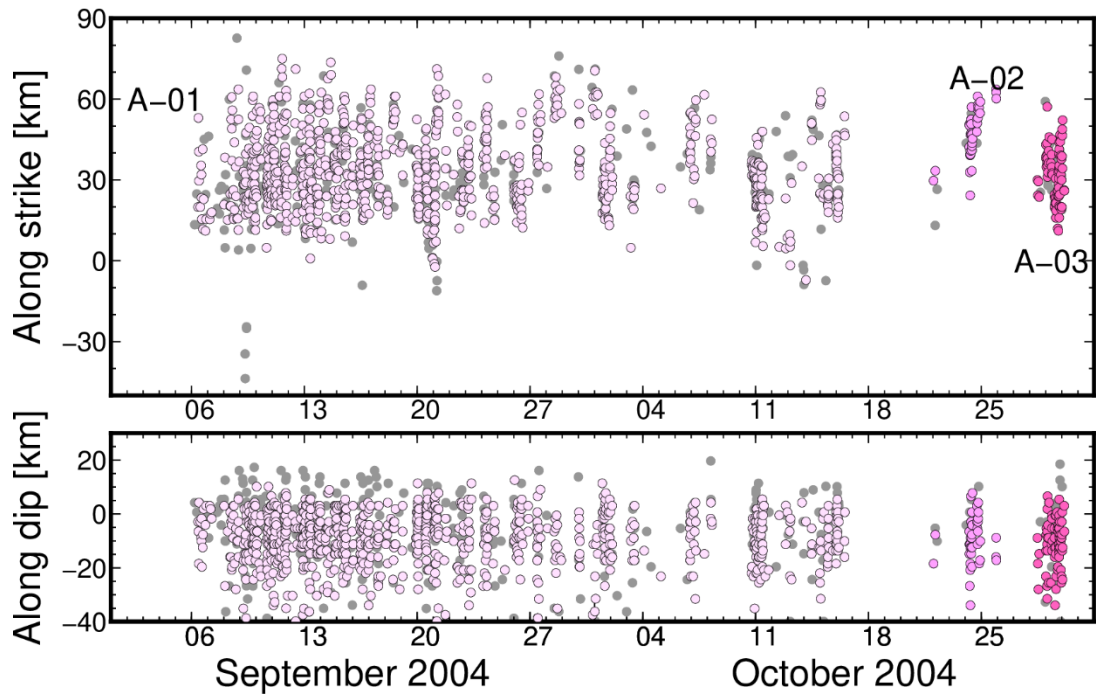


Figure S4. Spatiotemporal variations of shallow VLFs during swarms A-01, 02, and 03. Gray circles indicate the shallow VLFs with VR < 30%.

Table S1. List of the detected shallow VLFE swarms in this study. Durations of the swarms are times between the initial and final shallow VLFEs in each swarm. The areas and cumulative moments were evaluated using shallow VLFEs with VRs equal to or greater than 30%.

Index	Initial date (JST)	Duration [s]	Areas [m ²]	Along-strike dist. [m]	Cum. Moment [Nm]
A-01	2004-09-06T04:40:12.00	3485898.0	3.59E+09	82153.8	1.38E+18
A-02	2004-10-22T00:58:02.50	336205.0	9.28E+08	39336.1	5.14E+16
A-03	2004-10-28T11:46:34.00	360075.5	1.79E+09	63303.8	8.26E+16
A-04	2004-11-13T00:07:21.00	264886.0	1.17E+09	47603.7	5.12E+16
A-05	2004-12-13T02:26:08.50	180772.0	1.18E+09	50479.7	1.17E+17
A-06	2004-12-27T02:52:39.00	328496.5	2.55E+08	19132.6	4.00E+16
A-07	2005-08-29T00:28:33.50	366288.0	9.94E+08	34807.2	9.46E+16
A-08	2007-07-21T04:13:54.00	326033.5	9.12E+08	37379.0	1.71E+16
A-09	2009-03-24T04:16:39.00	959886.5	2.78E+09	79642.1	3.11E+17
A-10	2009-04-08T21:09:14.50	347819.0	8.23E+08	32544.7	2.98E+16
A-11	2009-04-27T14:11:43.50	97245.5	1.64E+08	7415.6	1.24E+16
A-12	2016-04-03T07:01:47.00	731415.5	7.43E+08	30236.3	4.18E+16
A-13	2018-05-03T11:06:20.50	100466.0	6.13E+07	7417.1	2.38E+15
A-14	2020-12-06T21:12:18.50	1458580.0	2.68E+09	69854.3	2.92E+17
A-15	2020-12-28T12:49:51.50	153422.5	1.10E+09	42753.7	5.73E+16
A-16	2021-01-12T04:13:09.00	179378.0	5.23E+08	27757.4	1.16E+16
B-01	2004-04-29T21:53:19.00	1517602.5	3.28E+08	32067.2	1.30E+16
B-02	2008-03-23T01:07:54.00	1120895.0	1.46E+08	15425.3	5.00E+15
B-03	2016-04-06T07:12:00.00	360198.0	6.15E+07	9684.3	2.70E+15
B-04	2020-12-30T23:24:55.00	1229535.5	4.08E+08	40898.4	6.21E+15
C-01	2004-09-06T15:03:51.50	2418988.5	1.77E+09	90990.3	5.88E+16
C-02	2004-10-31T22:04:16.50	3341780.0	3.05E+08	35122.4	5.83E+15
C-03	2006-08-19T00:31:25.00	1674820.5	1.46E+08	8947.2	1.02E+16
C-04	2009-03-19T01:17:53.50	10884568.5	5.15E+09	102606.0	1.44E+17
C-05	2010-01-13T04:29:05.00	5602565.0	1.56E+09	61370.3	1.50E+16
C-06	2011-03-08T21:28:16.00	2567116.5	3.76E+09	113715.0	2.87E+16
C-07	2014-12-01T18:28:55.50	974671.0	2.02E+08	10625.4	2.35E+16
C-08	2015-08-25T16:45:28.50	2686835.0	1.91E+08	15826.8	3.00E+16
C-09	2018-02-28T08:27:26.00	7952416.0	3.12E+09	80469.0	1.35E+17

Table S2. Comparisons of seismic moments between shallow SSEs and VLFE swarms.

Period	Reg.	Mo of Shallow SSE [Nm]	Reference of shallow SSEs	Cum. Mo of shallow VLFEs [Nm]	VLFE swarms index	VLEs/SSEs [%]
March 2009~ July 2009	C	2.51×10^{18}	Yokota & Ishikawa, 2020	1.44×10^{17}	C-04	5.7
April 2016	A	2.51×10^{18}	Itaba, 2018	0.46×10^{17}	A-12 and B-03	1.8
March 2018~ May 2018	C	10.0×10^{18}	Yokota & Ishikawa, 2020	1.34×10^{17}	C-09	1.3
Dec. 2020~ Jan. 2021	A	$2.5 \sim 10.0 \times 10^{18}$	Geological Survey of Japan AIST, 2021	3.67×10^{17}	A-14, 15, 16, and B-04	3.6~14.7

References of supporting information

- DeMets, C., Gordon, R. G., & Argus, D. F. (2010). Geologically current plate motions. *Geophysical Journal International*, 181(1), 1–80. <https://doi.org/10.1111/j.1365-246X.2009.04491.x>
- Geological Survey of Japan, N. I. of A. I. S. and T., & National Research Institute for Earth Science and Disaster Resilience. (2021, September). Short-term slow slip events in the Tokai area, the Kii Peninsula and the Shikoku District, Japan (from November 2020 to April 2021). Retrieved November 8, 2021, from https://cais.gsi.go.jp/YOCHIREN/report/kaihou106/06_03.pdf
- Itaba, S. (2018). *Detection of shallow SSE Off the Kii Peninsula by an onland borehole strain observation network*. Retrieved from http://www.tries.jp/research/doc/2018061416302928_22.pdf
- Koketsu, K., Miyake, H., & Suzuki, H. (2012). Japan Integrated Velocity Structure Model Version 1. *Proceedings of the 15th World Conference on Earthquake Engineering*, 1–4.
- Maeda, T., Takemura, S., & Furumura, T. (2017). OpenSWPC: an open-source integrated parallel simulation code for modeling seismic wave propagation in 3D heterogeneous viscoelastic media. *Earth, Planets and Space*, 69(1), 102. <https://doi.org/10.1186/s40623-017-0687-2>
- National Research Institute for Earth Science and Disaster Resilience. (2019). NIED Hi-net. <https://doi.org/10.17598/NIED.0003>
- Nishida, K. (2017). Ambient seismic wave field. *Proceedings of the Japan Academy, Series B*, 93(7), 423–448. <https://doi.org/10.2183/pjab.93.026>
- Sugioka, H., Okamoto, T., Nakamura, T., Ishihara, Y., Ito, A., Obana, K., et al. (2012). Tsunamigenic potential of the shallow subduction plate boundary inferred from slow seismic slip. *Nature Geoscience*, 5(6), 414–418. <https://doi.org/10.1038/ngeo1466>
- Takemura, S., Matsuzawa, T., Kimura, T., Tonegawa, T., & Shiomi, K. (2018). Centroid Moment Tensor Inversion of Shallow Very Low Frequency Earthquakes Off the Kii Peninsula, Japan, Using a Three-Dimensional Velocity Structure Model. *Geophysical Research Letters*, 45(13), 6450–6458. <https://doi.org/10.1029/2018GL078455>
- Takemura, S., Noda, A., Kubota, T., Asano, Y., Matsuzawa, T., & Shiomi, K. (2019). Migrations and Clusters of Shallow Very Low Frequency Earthquakes in the Regions Surrounding Shear Stress Accumulation Peaks Along the Nankai Trough.

- Geophysical Research Letters*, 46(21), 11830–11840.
<https://doi.org/10.1029/2019GL084666>
- Takemura, S., Matsuzawa, T., Noda, A., Tonegawa, T., Asano, Y., Kimura, T., & Shiomi, K. (2019). Structural Characteristics of the Nankai Trough Shallow Plate Boundary Inferred From Shallow Very Low Frequency Earthquakes. *Geophysical Research Letters*, 46(8), 4192–4201. <https://doi.org/10.1029/2019GL082448>
- Takemura, S., Yabe, S., & Emoto, K. (2020). Modelling high-frequency seismograms at ocean bottom seismometers: effects of heterogeneous structures on source parameter estimation for small offshore earthquakes and shallow low-frequency tremors. *Geophysical Journal International*, 223(3), 1708–1723.
<https://doi.org/10.1093/gji/ggaa404>
- Takemura, S., Obara, K., Shiomi, K., & Baba, S. (2021). Spatiotemporal variations of shallow very low frequency earthquake activity southeast off the Kii Peninsula, along the Nankai Trough, Japan. *ESSOAr*.
<https://doi.org/10.1002/essoar.10507824.1>
- Tocheport, A., Rivera, L., & Chevrot, S. (2007). A systematic study of source time functions and moment tensors of intermediate and deep earthquakes. *Journal of Geophysical Research: Solid Earth*, 112(7), 1–22.
<https://doi.org/10.1029/2006JB004534>
- Tonegawa, T., Araki, E., Kimura, T., Nakamura, T., Nakano, M., & Suzuki, K. (2017). Sporadic low-velocity volumes spatially correlate with shallow very low frequency earthquake clusters. *Nature Communications*, 8(1), 2048.
<https://doi.org/10.1038/s41467-017-02276-8>
- Yabe, S., Baba, S., Tonegawa, T., Nakano, M., & Takemura, S. (2021). Seismic energy radiation and along-strike heterogeneities of shallow tectonic tremors at the Nankai Trough and Japan Trench. *Tectonophysics*, 800, 228714.
<https://doi.org/10.1016/j.tecto.2020.228714>
- Yokota, Y., & Ishikawa, T. (2020). Shallow slow slip events along the Nankai Trough detected by GNSS-A. *Science Advances*, 6(3), eaay5786.
<https://doi.org/10.1126/sciadv.aay5786>